Am J Transl Res 2019;11(5):3018-3028
www.ajtr.org /ISSN:1943-8141/AJTR0086848

Original Article

A novel human-derived tissue-engineered patch for vascular reconstruction

Liping Gao[1,2], Tianming Shi[3], Zhenhua Wang[4], Jingjing Lv[5], Sebastian Schmull[6], Hong Sun[1,2]

[1]Department of Physiology, Xuzhou Medical University, Xuzhou, Jiangsu Province, China; [2]National Demonstration Center for Experiment Basic Medical Science Education, Xuzhou Medical University, Xuzhou, Jiangsu Province, China; [3]Department of Gynecology, International Peace Maternal and Child Health Care Hospital, School of Medicine, Shanghai Jiao Tong University, Shanghai, China; [4]Department of Cardiovascular Surgery, Ren Ji Hospital, School of Medicine, Shanghai Jiao Tong University, Shanghai, China; [5]Department of Cardiothoracic Surgery, Heart Center, Shanghai Children's Medical Center, School of Medicine, Shanghai Jiao Tong University, Shanghai, China; [6]Renji-Med X Clinical Stem Cell Research Center, Ren Ji Hospital, School of Medicine, Shanghai Jiao Tong University, Shanghai, China

Received October 16, 2018; Accepted March 16, 2019; Epub May 15, 2019; Published May 30, 2019

Abstract: Vascular patches are commonly applied in tissue repair and reconstruction in congenital cardiac surgery. However, the currently available patch materials are inappropriate to be used in the pediatric population due to their lack of supporting tissue growth potential. In our study an active patch material was developed by seeding pediatric patient's bone marrow stem cells on a decellularized aortic extracellular matrix (ECM) scaffold. The patch was then implanted to repair abdominal aorta defects of nude rats. Two months after implantation, tissue remodeling, vascular cell regeneration, and cellular integration were investigated using histology and fluorescent staining. Histology demonstrated infiltration of host cells and formation of organized cell layers as well as intact collagen and elastic fibers inside the patch material. Immunofluorescence indicated regeneration of endothelial and smooth muscle cells. Liquid chromatography-tandem mass spectrometry (LC-MS/MS) identified multiple vascularization-promoting components and growth factors in decellularized aortic ECM scaffold. These results demonstrated growth potential and suitability of human derived tissue-engineered patch for vascular reconstruction, and thus, it might be considered in the future as treatment option in pediatric patients.

Keywords: Tissue-engineered vascular patch, extracellular matrix, implantation, remodeling, vascularization

Introduction

Vascular patches are commonly applied in tissue repair and reconstruction in congenital cardiac surgery, including pulmonary arterioplasty, right ventricular outflow tract patch, valve leaflet augmentation, repair of unroofed coronary sinus etc [1]. While providing mechanical support, a favorable vascular patch would facilitate potential remodeling or even tissue regeneration, and finally transform into mature vascular tissue. Such a patch is especially suitable to pediatric patients in that it can grow inside the body as the child grows. However, the used synthetic patch materials require multiple operations in the pediatric population due to the lack of growth potential [2]. Biological materials show approximate characteristics of the native tissue, and thus, are considered as an alternative to synthetic materials [3]. Currently, widely applied ECM materials in cardiac surgery are derived from the porcine small intestinal submucosa (SIS). Although the tissue remodeling and regeneration of this material has been demonstrated in preclinical experiments [4-6], clinical outcomes indicated that the porcine SIS was not remodeled into tissue which resembles a native tissue at 9 months after implantation in patients with congenital heart defects [7].

We have constructed a tissue-engineered vascular patch (TEVP) using decellularized extracellular matrix (ECM) obtained from excised human aorta during surgery [8]. In vitro experiments have demonstrated that the decellularized ECM scaffold retained native extracellular

matrix composition, similar mechanical performance to native aortic tissue, and excellent biocompatibility. More important, the human-derived ECM scaffold provided a microenvironment which promoted growth and proliferation of bone marrow-derived progenitor cells. This preliminary pilot study gave early evidence that the decellularized aortic ECM could be used as a possible patch material *in vivo*.

In this study, we observed the effect of human-derived vascular patch on the repair of arterial defects and evaluated its remodeling potential *in vivo*. The vascular patches were implanted on the abdominal aorta of nude rats. Two months after implantation, tissue remodeling, vascular cell regeneration, and cellular integration were investigated by histological, immunohistochemical and immunofluorescentstaining. Capillary regeneration inside the patch was also detected. It was hypothesized that this human-derived vascular patch would show vascular cell regeneration, capillary formation, and overall integration with host tissue. This is the first study to construct, characterize, and perform an *in vivo* research on a human-derived vascular patch.

Materials and methods

Preparation of decellularized human aortic ECM scaffold

Human aortic tissues were collected during aorta replacement surgery for patients at the Department of Cardiac Surgery of Renji Hospital, Shanghai, China. The patients' information was listed in Table S1. The use of the patients' aortic tissues was approved by the ethics committee of Renji Hospital (permit number: 2012027), and written informed consent was obtained. Human aortic tissues were immediately washed three times in ice-cold phosphate-buffered saline to remove plasma and quickly cut into 1 cm × 1 cm pieces. Then, tissue pieces were embedded in O.C.T. (Sakura Finetek USA Inc., CA, USA) and frozen at -80°C for 2 hours. The pieces were cut into 200-μm thick sections, incubated with 0.5% sodium dodecyl sulfate (SDS; Sigma, USA) in deionized water and mildly vortexed at 37°C for 24 h. Hereafter, samples were incubated in 200 IU/ml Dnase I (Roche, Basel, Switzerland) solution to ensure removal of residual DNA. After lyophilization in a vacuum freeze-drier (Virtis Benchtop 6.6, SP Industries, Gardiner, NY), aortic ECM scaffolds were disinfected in 75% ethanol for 2 hours and stored at 4°C until use.

Isolation of bone marrow CD34+ progenitor cells and preparation of vascular patch

Use of bone marrow was approved by the Institutional Review Board of Shanghai Children's Medical Center, and written informed consent was obtained from parents of pediatric patients (permit number: SCMCIRB-K2016025). The pediatric patients' information was listed in Table S2. Bone marrow aspirates (1-2 ml) were obtained from pediatric patients with congenital heart disease. Bone marrow mononuclear cells were isolated by density gradient sedimentation with Human Lymphocyte Separation Medium (Biosera, England, UK). CD34+ progenitor cells were isolated by labeling bone marrow mononuclear cells with anti-CD34 antibody (Miltenyi Biotec, Germany) conjugated with magnetic beads. A different anti-CD34 antibody targeting another epitope (Biolegend, CA, USA) was used to confirm the enrichment of CD34+ progenitor cells. After moistening lyophilized tissue in distilled water, the 1 cm × 1 cm scaffolds were placed in a 24-well plate. For cell seeding on aortic ECM scaffold, 100 μl CD34+ cell suspension (2×10^5 cells) was added dropwise onto the surface of each scaffold, allowing cells to distribute throughout the scaffold. In order to enable the cells to attach to the scaffolds, cell-seeded ECM scaffolds were kept at 37°C in CO_2 incubator for 2 h. As control, 2×10^5 cells were seeded in culture plates coated with matrigel or fibronectin.

In vitro differentiation of CD34+ progenitor cells on scaffolds

The cultured cells on fibronectin, Matrigel, or ECM scaffolds were fixed in 4% paraformaldehyde for 15 min and were immersed in 0.5% Triton X-100 for 15 min, followed by blocking with 5% normal donkey serum for 1 h and overnight incubation at 4°C with rabbit anti-CD31 (Santa Cruz Biotechnology, TX, USA) or goat anti α-SMA (Abcam, Cambridge, UK) antibodies. Hereafter, the following secondary antibodies (Life Technologies, USA) were added and incubated for 1 h: donkey anti-rabbit Alexa 594 or donkey anti-goat Alexa 488. Cell nuclei were counterstained using DAPI. Cells were rinsed, cover-slipped, and fluorescence observed under a Nikon fluorescence microscope.

Implantation of vascular patch into nude rats

To observe the effect on the repair of abdominal aorta defect and to determine the remodeling *in vivo*, ECM scaffolds and human-derived vascular patches were implanted into nude rats, 3-4 month old, weighing 300 g (Charles River Laboratories, Boston, MA), as abdominal aorta interposition grafts. Briefly, nude rats were divided randomly into 3 groups: sham group, scaffold group (only decellularized aortic ECM was implanted), and patch group (vascular patch was implanted). All rats were anesthetized with 10% chloral hydrate (300 mg/kg), and 1-3% isoflurane was administrated via nose to maintain the anesthesia condition during operation. Animals were opened with a midline abdominal incision and the abdominal aorta between the renal artery and the inferior mesenteric artery was exposed under sterile conditions. The aortic branches in this segment were ligated with 9-0 suture and the proximal and distal portions of the aorta were clamped. The introduced defect was 3 mm in length. The vascular clamps were then removed and blood flow was checked. No blood leakage was confirmed before skin closure. The vascular patch was sutured over the defect using 10-0 monofilament nylon suture. After confirmation of blood flow and no present blood leakage, the skin incision was closed. Animals were allowed to recover from surgery and maintained in the absence of anti-coagulants for up to 2 months post operation.

Histological and immunofluorescence staining

Two months after implantation, vascular patches were removed. Subsequently, native aortas, ECM scaffolds, and vascular patches were fixed in 4% paraformaldehyde, embedded in paraffin, and cut into 5-μm sections. Sections were stained with hematoxylin and eosin (H&E), Van Gieson, Verhoeff's Van Gieson, and 4',6-diamidino-2-phenylindole (DAPI). For immunofluorescence staining, samples were embedded in O.C.T. (Sakura Finetek USA Inc., CA, USA) and frozen at -80°C for 2 hours. Then, samples were cut to a thickness of 5 μm using a freezing microtome. Samples were stained with antibodies against CD31 and α-SMA, as described in Subsection 2.3.

Label-free liquid chromatography-tandem mass spectrometry (LC-MS/MS)

The decellularized aortic ECM was grinded, homogenized in 8 mM urea, 10 mM dithiothreitol (DTT), 100 mM Tris (pH 8.0), and protease inhibitor, and then sonicated on ice for 60 s. After centrifugation at 10,000 g for 30 min, the supernatant was collected and protein concentrations were determined using Bradford Assay (Thermo Fisher Scientific, U.S.A). The sample was digested with trypsin for at least 12 h at 37°C at 1:100 enzyme-to-protein ratios. Digested proteins were then separated on a nanoflow Easy-nLC system (Thermo Scientific) and analyzed in triplicate on a Q-Exactive (Thermo Finnigan). The identified proteins were listed in Table S3. Data analysis was performed using Proteome Discoverer 1.4 (Thermo Scientific) and Mascot 2.2 (Matrix Science, London, UK) Software based on uniprot-human proteome database.

Statistical analysis

For all quantitative data, Student's t test was employed to examine the difference between two groups. GraphPad prism 5.0 software (GraphPad Software, Inc.CA, USA) was used for statistical analysis. Data were presented as mean ± standard deviation. A value of $P < 0.05$ was set to indicate statistically significance.

Results

Decellularized aortic ECM scaffold promotes CD34+ cell growth and proliferation in vitro

Human aortas were obtained from surgical explants and were sliced into 50-μm thick sheets, which were used for *in vitro* experiments. HE staining showed that cell nuclei were completely removed while ECM was reserved after decellularization process (**Figure 1A**, **1B**). To assess the cell growth and proliferation capabilities on the scaffold, CD34+ cells (1×10^5 cells/cm^2) were seeded on human aortic ECM scaffold. CD34+ cells adhered to the scaffold and grew well. The number of CD34+ cells significantly increased after culture for 5 days (**Figure 1C-E**).

Induction of differentiation of CD34+ cells in vitro into endothelial and SMC lineages

To investigate the potential of inductive differentiation, aortic ECM scaffold was seeded with CD34+ cells. At 14 d, the cells showed positive staining for EC marker CD31 (red) and SMC marker α-SMA (green), as indicated by immunofluorescence images. In contrast, after culture

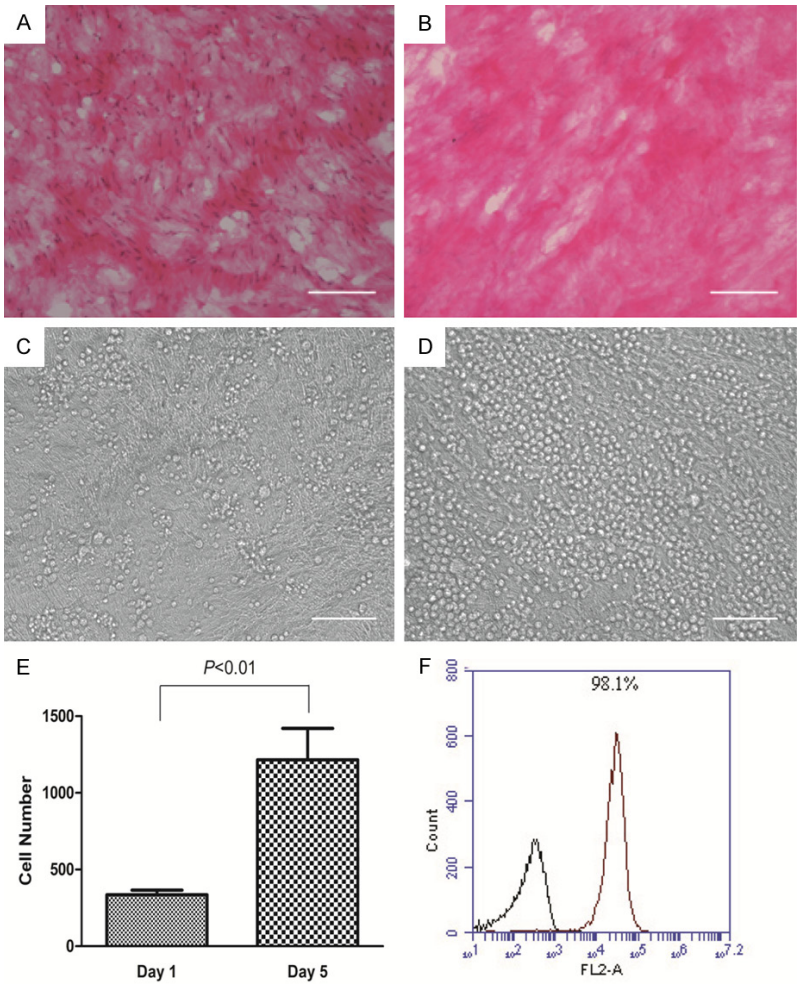

Figure 1. Decellularized aortic ECM scaffold and its facilitation on cell's proliferation. (A, B) H&E staining shows that cell nuclei (blue) were present in the undecellularized aortic tissue (A) but were absent in the decellularized aortic ECM scaffold (B), and aortic ECM is preserved after decellularization process. (C, D) show representative images of CD34+ progenitor cells cultured on the aortic ECM scaffold on day 1 (C) and day 5 (D) under optical microscope. (E) CD34+ progenitor cell number was significantly increased on day 5 compared with that on day 1 ($P < 0.01$), mean of 2 fields per scaffold, n = 3 representative pictures. (F) Flow cytometry shows the purity of CD34+ progenitor cell population reaches 98.1% using a different anti-CD34 antibody.

on Matrigel or fibronectin for 14 d, the cells only exhibited weak positive results for EC or SMC markers (**Figure 2**). These data indicated that aortic ECM scaffold is more conductive to induct CD34+ cells into vascular cells than Matrigel and fibronectin.

Vascular patch repaired abdominal aorta defect

Vascular patch was surgically implanted into nude rat abdominal aorta (**Figure 3A-D**). No blood leakage was observed after clamp removal. After 2 months post-surgery, 100% of nude rats with patch were alive, and no thrombosis was seen in explants for all groups. A portion of the aorta along with the patch was harvested and used as baseline control.

In vivo remodeling of vascular patch

After two months of implantation, H&E staining demonstrated that the cells infiltrated into the inside of the explanted ECM scaffold, but they arranged irregularly and did not form clear layers, as indicated in **Figure 4B**. In comparison, the cells inside the vascular patch were organized, and no major congregation of giant cells and macrophages was observed, which was similar to native arterial wall in control group. As shown in **Figure 4E**, **4F** and **4J**, Masson staining indicated that the vascular patch had a lower amount of collagen when compared to decellularized scaffold, suggesting an important role of seeded cells in reducing fibrosis. Van Gieson's staining, as shown in **Figure 4**, demonstrated that elastin in vascular patch group exhibited regular and continuous arrangement while fractured elastin could be found in decellularized scaffold.

After 2 months the animals with decellularized scaffold showed significant cell infiltration into the scaffold material, but cells present on the lumen side of the scaffold stained negative for CD31 which indicated endothelial cell deficiency. However, the cells lining the lumen of vascular patch stained positive, which was comparable to native vessels, indicating the regeneration of endothelial cells (**Figure 5A-C**). The green fluorescencent labeled α-SMA demonstrat-

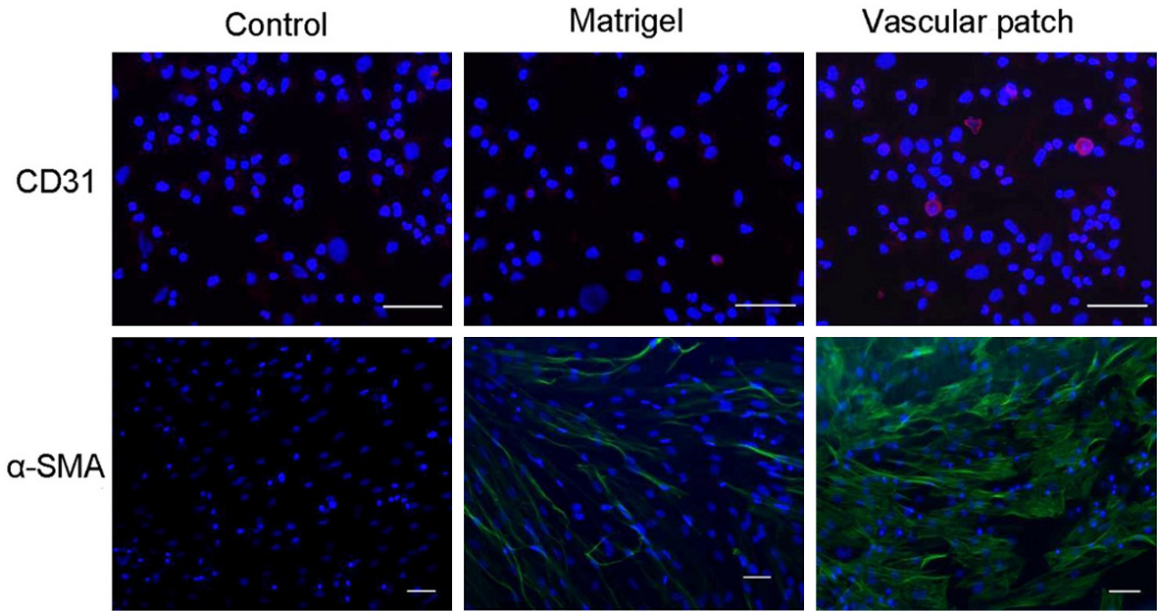

Figure 2. In vitro differentiation of CD34+ cells into ECs and SMCs inside vascular patch. Representative images of immunofluorescence staining with CD31 antibody (red) and α-SMA antibody (green) after CD34+ progenitor cells were cultured for 14 days on different scaffolds. Compared with control or matrigel group, more CD31-positive and α-SMA CD34+ cells were found in vascular patch group, which indicated that CD34+ cells are more inclined to differentiated into vascular ECs or SMCs when seeded on aortic ECM scaffold. DAPI (blue) was used for nuclei staining. Scale bar is 100 μm.

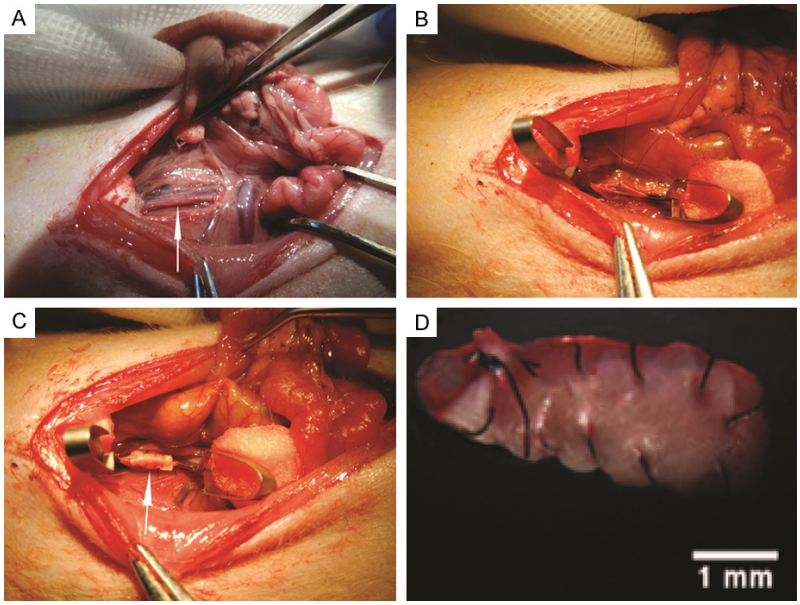

Figure 3. The process of vascular patch implantation on the abdominal aorta of nude rats. A. The white arrow indicates isolated abdominal aorta of nude rats. B. The isolated abdominal aorta was occluded with artery clamp on both sides, and then a piece of aortic wall (3 mm in length and 0.5 mm in width) was cut off, leading to abdominal aorta defect. C. The abdominal aorta defect was repaired with vascular patch in vivo. D. Two months post-implantation, the whole vascular patch was explanted and photographed under stereo microscope.

ed that smooth muscle cells have populated the vascular patch, though there are still some differences in smooth muscle cell orientation compared to control animal's native vessel. As a comparison, the decellularized scaffold also exhibited smooth muscle cell regeneration but that appeared to be unorganized after implantation for 2 months (**Figure 5D-F**).

Vascularization-related proteins and growth factors in decellularized human aortic ECM scaffold

Human aortic ECM proteins were extracted and then identified by label-free LC-MS/MS. A total of 1172 proteins were identified and 23 proteins associated with vessel formation were also detected (**Figure 6A**, **6B**). These 23 proteins included proteoglycans and glycoproteins (decorin, fibrillin, fibulin-1, galectin, tenascin-X, and vitronectin) and the basement membrane proteins collagen

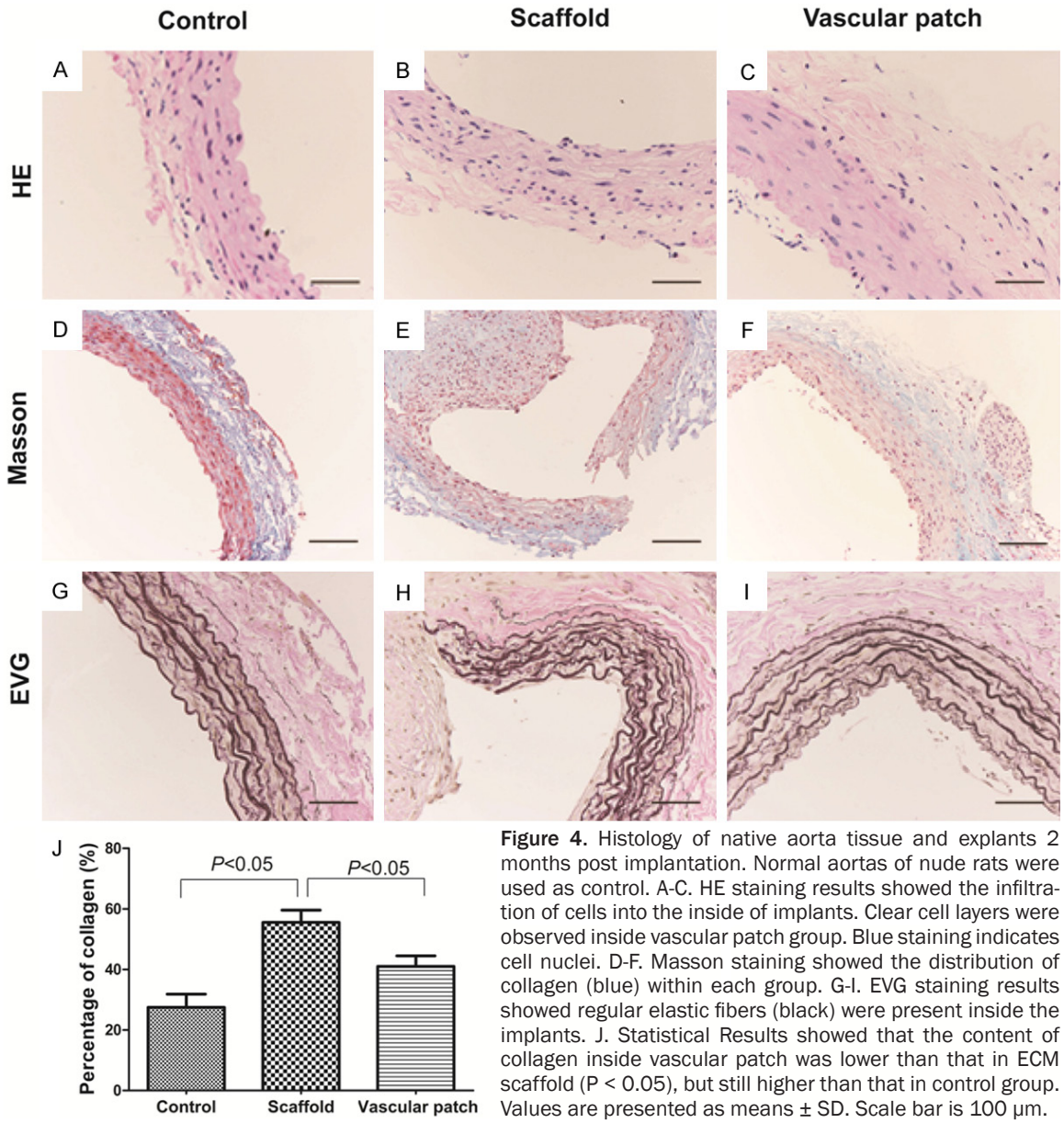

Figure 4. Histology of native aorta tissue and explants 2 months post implantation. Normal aortas of nude rats were used as control. A-C. HE staining results showed the infiltration of cells into the inside of implants. Clear cell layers were observed inside vascular patch group. Blue staining indicates cell nuclei. D-F. Masson staining showed the distribution of collagen (blue) within each group. G-I. EVG staining results showed regular elastic fibers (black) were present inside the implants. J. Statistical Results showed that the content of collagen inside vascular patch was lower than that in ECM scaffold ($P < 0.05$), but still higher than that in control group. Values are presented as means ± SD. Scale bar is 100 μm.

(COL I A1, COL I A2, COL III A1, COL IV A1, COL IV A2, COL IV A3, COL XV A1, and COL XVIII A1), fibronectin (fibronectin-1 and fibronectin-III), laminin (laminin A2, laminin A4, laminin A5, and laminin B2), plectin, fibrinogen, and perlecan, each of which has been shown to promote vessel formation. Additionally, nine growth factors were identified, including multiple epidermal growth factor-like domains protein 6, platelet derived growth factor C, platelet derived growth factor D, platelet derived growth factor alpha polypeptide, hepatocyte growth factor-like protein, transforming growth factor (beta-1 and beta-2), connective tissue growth factor, and fibroblast growth factor 14 (**Table 1**).

Discussion

Multiple biological materials have been used to repair and reconstruct damaged vessels [9, 10]. Ideally, they should mimic the native vessel structure as closely as possible [11]. The use of decellularized blood vessels is advantageous due to its similar mechanical characteristics and structural elements to native vascular tissue. In this paper, a vascular patch was prepared from human decellularized arterial tissue seeded with bone marrow stem cells. In a previous study, the vascular patch has been demonstrated to possess the original three-dimensional structure and biochemical properties as

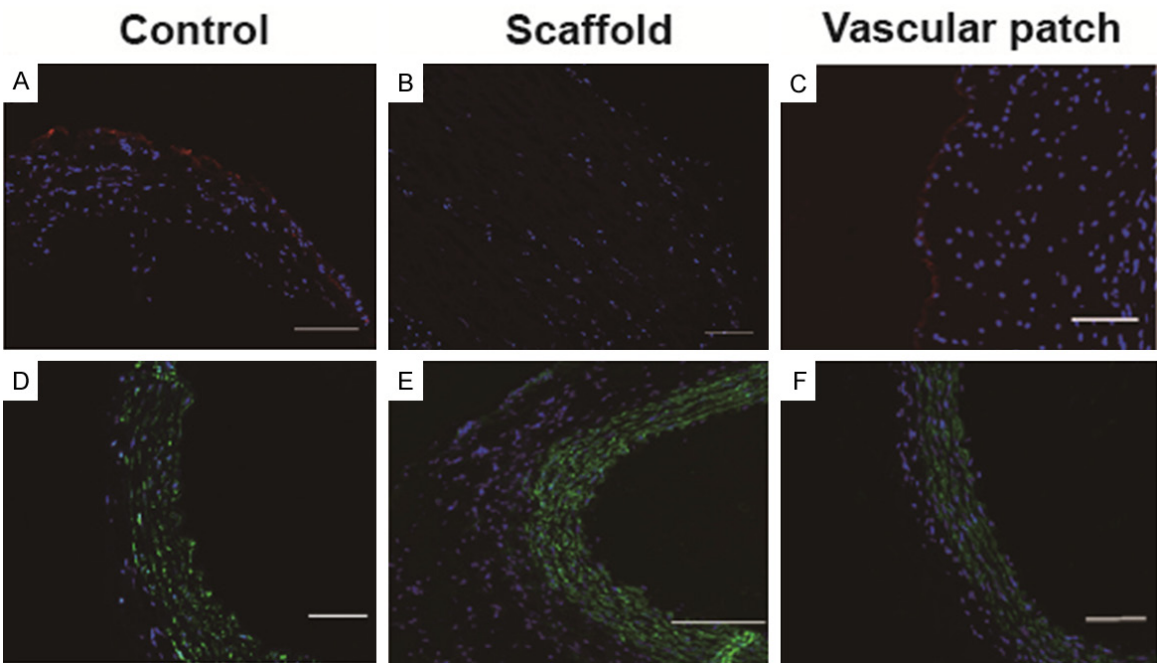

Figure 5. Representative images of Immunofluorescence staining for each group. A. CD31 staining of normal rat aortic tissue demonstrating the coverage of an intact layer of endothelial cells on the inner surface of the blood vessel. B. No endothelial cell was found on the inner surface of the decellularized ECM scaffold 2 months post in vivo implantation. C. CD31 staining of tissue-engineered vascular patch indicating the retention of endothelial cells. D. α-SMA staining of normal rat aortic tissue. E. Increased brand of α-SMA staining disclosing excessive regeneration of smooth muscle cells in scaffold without cell seeding. F. α-SMA staining of tissue-engineered vascular patch indicating the moderate regeneration of smooth muscle cells. The nuclei were stained blue by DAPI. Scale bar is 100 μm.

well as good biocompatibility as the native aorta [8]. When implanted into nude rats, the vascular patch was shown to repair abdominal aorta defect while allowing endothelial and smooth muscle cell regrowth. Additionally, when the vascular patch was subcutaneously implanted into nude mice, it promoted formation of functional neomicrovessels inside the material (data not shown). These results indicated that the vascular patch achieved constructive remodeling and integrated with the host vascular tissue *in vivo*.

To identify the ability of the vascular patch to integrate with the host vessel wall, a long term *in vivo* study was performed. The operation procedures showed that the vascular patch could be easily handled in surgery and had favorable suture strength. Moreover, the vascular patch mended the defective abdominal aorta with no blood leakage and was able to withstand rat abdominal aorta pressure which is similar to human's arterial pressure [12]. Of note, the patch was still in place when it was explanted.

The histological results demonstrated that although most host cells immigrated into the inside of implants, there were still structural differences between the decellularized scaffold and vascular patch. HE staining showed that the cells inside vascular patch were more homogeneous and organized than those in decellularized scaffold, and they formed clear cell layers similar to the native vessel as shown in **Figure 4A-C**. Masson trichrome disclosed that the vascular patch had more collagen than the native vessel, but still less than the decellularized scaffold, which suggested that excessive collagen hyperplasia was not present in vascular patch. Furthermore, the elastin fibers were continuous and intact inside the vascular patch. These results suggested that repopulation by stem cells on acellular ECM promoted the implants to integrate into host tissues, facilitating both constructive remodeling and regeneration process. This is in line with other investigations. Ross et al and others also found that matrix-cell interaction in acellular scaffolds not only induced differentiation of seeded

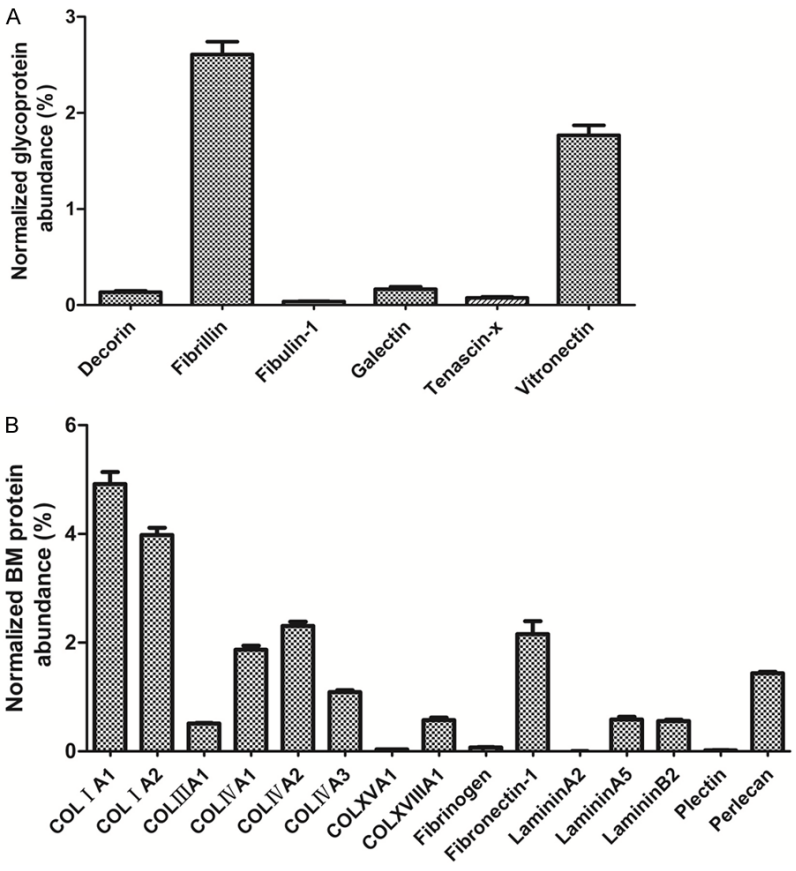

Figure 6. Vasculogenesis-promoting proteins analysis of decellularized human aortic ECM. Data was normalized on a scale ranging from 0% to 100%. Normalized abundance (%) of vasculogenesis-related glycoproteins (A) and basement membrane proteins (B) were determined using LC-MS/MS. Data determined by label-free LC-MS/MS and are representative of 3 biological replicates.

cells, but also support remodeling of scaffolds and replacing the original matrix [13, 14].

CD31 staining confirmed the appearance of an endothelial cell layer covering the vascular patch, giving evidence that the vascular patch *in vivo* remodeled into native vessel. The presence of an endothelial cell layer is important as it provides a non-contacting barrier with blood on the surface of the vascular patch. Achievement of re-endothelialization on an implanted graft is thought to be crucial in the prevention of complications such as intimal hyperplasia and thrombogenicity [15]. Also, the vascular patch had integration of smooth muscle cells arranging in a pattern similar to native tissue in the scaffold, as indicated by immunofluorescence staining in **Figure 5**. Smooth muscle cells play a major role in vascular remodeling and ECM synthesis, as well as maintenance of a functional endothelium [16, 17], giving further evidence that our human-derived patch is supportive to vascular regeneration *in vivo*.

It is well established that ECM facilitates constructive tissue remodeling and release of growth factors from ECM and vascularization-promoting components in ECM are likely mechanisms of action [9, 18]. We thus analyzed the chemical composition of the human aortic ECM by LSMS/MS. In general, biological ECM components contain both vascularization-promoting proteins and anti-vasculogenesis proteins. Consistent with the findings of a previous study [19], the LS-MS/MS results indicated that decellularized human aortic ECM contained a large number of vascularization-promoting proteins, including decorin, fibrillin, fibulin-1, galectin, tenascin-X, vitronectin, collagen, and fibronectin. It was shown that these vascularization-promoting proteins play important roles during the process of initiating vascularization (activating endothelial cells) [20]. Anti-vasculogenesis proteins within ECM include arrestin, canstatin, tumstatin, restin, endostatin, anastellin, endorepellin, elastin derived peptides, and thrombospondin [20-23]. However, only thrombospondin, a transient molecule, was detected indecellularized human aortic ECM. The dominant distribution of vascularization-promoting proteins may facilitate vasculogenesis inside human aortic ECM. In addition, several growth factors were also detected in aortic ECM, including platelet derived growth factor, transforming growth factor beta, hepatocyte growth factor, and connective tissue growth factor, which were shown to be in favor of vascularization [24-26]. Thus, mass spectrometry also indicates the suitability and beneficial effect of our human-derived vascular patch in supporting the local microenviron-

Table 1. Growth factors detected in human aortic decellularized ECM scaffold

Number	Accession	Genesymbol	Description
1	O75095	MEGF6	Multiple epidermal growth factor-like domains protein 6
2	B2R9K6	PDGFC	Platelet derived growth factor C
3	Q32M96	PDGFA	Platelet-derived growth factor alphapolypeptide
4	G3XAK1	MST1	Hepatocyte growth factor-like protein
5	Q9GZP0	PDGFD	Platelet-derived growth factor D
6	P01137	TGFB1	Transforming growth factor beta-1
7	B2RCP7	CTGF	Connective tissue growth factor
8	B2R7T2	TGFB2	Transforming growth factor, beta 2
9	Q92915	FGF14	Fibroblast growth factor 14

ment, e.g. tissue re-growth, remodeling, and neovessel formation.

It can be noted that the endothelial cell coverage on implants was only found in vascular patch group, but not in scaffold group, as demonstrated in **Figure 4**, suggesting the seeded CD34+ progenitor cells may play an important role in host vascular regeneration. However, previous studies reported that the seeded human cells onto the scaffold were lost within 1 week after implantation [27, 28]. Hibino N et al also confirmed that tissue-engineered vascular grafts form neovessels that arise from regeneration of the adjacent blood vessel [28]. Nevertheless, it was considered that the seeded cells onto scaffold promoted the regeneration of host vascular cells via a paracrine mechanism. Roh JD et al demonstrated that bone marrow mononuclear cells seeded onto vascular grafts mediated the vascular remodeling and development via paracrine mechanism although they disappeared in the early phase [29]. Based on these previous findings and the results of the present study, we speculate that the seeded CD34+ progenitor cells may promote the regeneration of tissue mediated by the human-derived patch *in vivo*.

The present study demonstrated that human-derived vascular patch not only repaired abdominal aorta defect but also achieved tissue remodeling and vascular regeneration in nude rats. It was shown that both aortic ECM components and the seeded CD34+ cells contribute to vascular regeneration mediated by human-derived patch. For clinical applicability, autologous CD34+ progenitor cells could be obtained from patient bone marrow as seeding cells to produce such a patient-specific vascular patch. Thus, the human-derived patch may represent an effective material for the repair of congenital heart and vascular diseases in children, so as to avoid the need of reoperation caused by the prosthetic material and the child growth mismatch. However, the study examined only a limited number of animals with a relative short time-course observation. Further investigation with a larger sample size and longer *in vivo* experiments are needed to allow comprehensive evaluations. Larger animal models will be additionally required to fully characterize the human-derived vascular patch because rodents and humans have different basal immune responses to pathogens [30], which may influence assessment of remodeling and regeneration.

Conclusion

This study examined the potential of a human-derived vascular patch for vascular repair application. The patches were capable of withstanding the high pressure inside the abdominal aorta and showing good mechanical property. The host cell infiltration and endothelial and smooth muscle cell regeneration demonstrated the potential of this patch to remodel and grow *in vivo*. Moreover, the potential to invoke vascularization is also extremely important for regenerative applications.

Acknowledgements

This study was supported by grants from the National Science Foundation of China (No. 81370329, No. 81461138036) (to Hong Sun). We thank Zhen-Hua Wang for his technical assistance.

Disclosure of conflict of interest

None.

Address correspondence to: Dr. Hong Sun, Department of Physiology, Xuzhou Medical University, 209 Tongshan Road, Xuzhou, Jiangsu Province, China. Tel: +86-516-83262618; Fax: +86-516-83262858; E-mail: sunh@xzhmu.edu.cn

References

[1] Holubec T, Caliskan E, Sundermann SH, Starck CT, Plass A, Bettex D, Falk V and Maisano F. Use of extracellular matrix patches in cardiac surgery. J Card Surg 2015; 30: 145-148.

[2] Shinoka T and Breuer C. Tissue-engineered blood vessels in pediatric cardiac surgery. Yale J Biol Med 2008; 81: 161-166.

[3] Bolland F, Korossis S, Wilshaw SP, Ingham E, Fisher J, Kearney JN and Southgate J. Development and characterisation of a full-thickness acellular porcine bladder matrix for tissue engineering. Biomaterials 2007; 28: 1061-1070.

[4] Wainwright JM, Hashizume R, Fujimoto KL, Remlinger NT, Pesyna C, Wagner WR, Tobita K, Gilbert TW and Badylak SF. Right ventricular outflow tract repair with a cardiac biologic scaffold. Cells Tissues Organs 2012; 195: 159-170.

[5] Mewhort HE, Turnbull JD, Meijndert HC, Ngu JM and Fedak PW. Epicardial infarct repair with basic fibroblast growth factor-enhanced CorMatrix-ECM biomaterial attenuates postischemic cardiac remodeling. J Thorac Cardiovasc Surg 2014; 147: 1650-1659.

[6] Badylak SF. The extracellular matrix as a biologic scaffold material. Biomaterials 2007; 28: 3587-3593.

[7] Zaidi AH, Nathan M, Emani S, Baird C, del Nido PJ, Gauvreau K, Harris M, Sanders SP and Padera RF. Preliminary experience with porcine intestinal submucosa (CorMatrix) for valve reconstruction in congenital heart disease: histologic evaluation of explanted valves. J Thorac Cardiovasc Surg 2014; 148: 2216-2214, 2225, e2211.

[8] Gao LP, Du MJ, Lv JJ, Schmull S, Huang RT and Li J. Use of human aortic extracellular matrix as a scaffold for construction of a patient-specific tissue engineered vascular patch. Biomed Mater 2017; 12: 065006.

[9] Muto A, Nishibe T, Dardik H and Dardik A. Patches for carotid artery endarterectomy: current materials and prospects. J Vasc Surg 2009; 50: 206-213.

[10] Cho SW, Park HJ, Ryu JH, Kim SH, Kim YH, Choi CY, Lee MJ, Kim JS, Jang IS, Kim DI and Kim BS. Vascular patches tissue-engineered with autologous bone marrow-derived cells and decellularized tissue matrices. Biomaterials 2005; 26: 1915-1924.

[11] Bordenave L, Menu P and Baquey C. Developments towards tissue-engineered, small-diameter arterial substitutes. Expert Rev Med Devices 2008; 5: 337-347.

[12] Waki H, Shimizu T, Katahira K, Nagayama T, Yamasaki M and Katsuda S. Effects of microgravity elicited by parabolic flight on abdominal aortic pressure and heart rate in rats. J Appl Physiol (1985) 2002; 93: 1893-1899.

[13] Ross EA, Abrahamson DR, St John P, Clapp WL, Williams MJ, Terada N, Hamazaki T, Ellison GW and Batich CD. Mouse stem cells seeded into decellularized rat kidney scaffolds endothelialize and remodel basement membranes. Organogenesis 2012; 8: 49-55.

[14] Kennedy KM, Bhaw-Luximon A and Jhurry D. Cell-matrix mechanical interaction in electrospun polymeric scaffolds for tissue engineering: Implications for scaffold design and performance. Acta Biomater 2017; 50: 41-55.

[15] Melchiorri AJ, Hibino N and Fisher JP. Strategies and techniques to enhance the in situ endothelialization of small-diameter biodegradable polymeric vascular grafts. Tissue Eng Part B Rev 2013; 19: 292-307.

[16] Wang Z, Wang DZ, Pipes GC and Olson EN. Myocardin is a master regulator of smooth muscle gene expression. Proc Natl Acad Sci U S A 2003; 100: 7129-7134.

[17] Newby AC and Zaltsman AB. Molecular mechanisms in intimal hyperplasia. J Pathol 2000; 190: 300-309.

[18] Wang W, Zhang X, Chao NN, Qin TW, Ding W, Zhang Y, Sang JW and Luo JC. Preparation and characterization of pro-angiogenic gel derived from small intestinal submucosa. Acta Biomater 2016; 29: 135-148.

[19] Hughes C, Radan L, Chang WY, Stanford WL, Betts DH, Postovit LM and Lajoie GA. Mass spectrometry-based proteomic analysis of the matrix microenvironment in pluripotent stem cell culture. Mol Cell Proteomics 2012; 11: 1924-1936.

[20] Neve A, Cantatore FP, Maruotti N, Corrado A and Ribatti D. Extracellular matrix modulates angiogenesis in physiological and pathological conditions. Biomed Res Int 2014; 2014: 756078.

[21] Sweeney SM, DiLullo G, Slater SJ, Martinez J, Iozzo RV, Lauer-Fields JL, Fields GB and San Antonio JD. Angiogenesis in collagen I requires alpha2beta1 ligation of a GFP*GER sequence and possibly p38 MAPK activation and focal adhesion disassembly. J Biol Chem 2003; 278: 30516-30524.

[22] Estrach S, Cailleteau L, Franco CA, Gerhardt H, Stefani C, Lemichez E, Gagnoux-Palacios L, Meneguzzi G and Mettouchi A. Laminin-binding integrins induce Dll4 expression and Notch signaling in endothelial cells. Circ Res 2011; 109: 172-182.

[23] Kim S, Bakre M, Yin H and Varner JA. Inhibition of endothelial cell survival and angiogenesis

by protein kinase A. J Clin Invest 2002; 110: 933-941.
[24] Badylak SF, Freytes DO and Gilbert TW. Reprint of: Extracellular matrix as a biological scaffold material: Structure and function. Acta Biomater 2015; 23 Suppl: S17-26.
[25] Morishita R, Aoki M, Hashiya N, Yamasaki K, Kurinami H, Shimizu S, Makino H, Takesya Y, Azuma J and Ogihara T. Therapeutic angiogenesis using hepatocyte growth factor (HGF). Curr Gene Ther 2004; 4: 199-206.
[26] Ponticos M. Connective tissue growth factor (CCN2) in blood vessels. Vascul Pharmacol 2013; 58: 189-193.
[27] Sugiura T, Hibino N, Breuer CK and Shinoka T. Tissue-engineered cardiac patch seeded with human induced pluripotent stem cell derived cardiomyocytes promoted the regeneration of host cardiomyocytes in a rat model. J Cardiothorac Surg 2016; 11: 163.
[28] Hibino N, Villalona G, Pietris N, Duncan DR, Schoffner A, Roh JD, Yi T, Dobrucki LW, Mejias D, Sawh-Martinez R, Harrington JK, Sinusas A, Krause DS, Kyriakides T, Saltzman WM, Pober JS, Shin'oka T and Breuer CK. Tissue-engineered vascular grafts form neovessels that arise from regeneration of the adjacent blood vessel. FASEB J 2011; 25: 2731-2739.
[29] Roh JD, Sawh-Martinez R, Brennan MP, Jay SM, Devine L, Rao DA, Yi T, Mirensky TL, Nalbandian A, Udelsman B, Hibino N, Shinoka T, Saltzman WM, Snyder E, Kyriakides TR, Pober JS and Breuer CK. Tissue-engineered vascular grafts transform into mature blood vessels via an inflammation-mediated process of vascular remodeling. Proc Natl Acad Sci U S A 2010; 107: 4669-4674.
[30] Tao L and Reese TA. Making mouse models that reflect human immune responses. Trends Immunol 2017; 38: 181-193.

Table S1. The information of patients who provided aortic tissues

Patient number	Sex	Age	Diagnosis	Sample
1	Male	60	Coronary disease	Aortic wall
2	Male	50	Coronary disease; inferior wall myocardial infarction	Aortic wall
3	Male	64	Coronary disease	Aortic wall
4	Female	59	Ascend aortic aneurysm; aortic regurgitation; mitral regurgitation; Bentall's operation	Ascending aortic wall
5	Male	60	Coronary disease; percutaneous coronary intervention (PCI) and Off-pump coronary artery bypass (OPCAB)	Aortic wall
6	Male	44	Aortic dissection (Debakey I)	Aortic wall
7	Female	27	Ascend aortic aneurysm; aortic insufficiency; Marfan syndrome	Aortic wall
8	Female	56	Aortic dissection (Debakey I)	Aortic wall

Table S2. The information of patients who provided bone marrow aspirates

Patient number	Hospitalization number	Sex	Age	Diagnosis
1	244856	Female	5 months	VSD
2	245262	Female	1 year 7 months	VSD
3	246452	Female	5 years	PAVC
4	246731	Female	2 years	ASD
5	247055	Male	1 years 7 months	TOF
6	247870	Male	3 years	VSD
7	248149	Male	10 months	VSD
8	248182	Male	1 year	VSD
9	248606	Male	1 years 2 months	TGA
10	249672	Female	3 months	VSD
11	249873	Male	1 year 5 months	VSD
12	249848	Male	6 months	VSD
13	250403	Male	2 years 7 months	VSD
14	250791	Female	1 year	VSD
15	251336	Male	4 years	ASD
16	257059	Male	3 years 5 months	ASD
17	254743	Female	6 months	ASD
18	255190	Male	7 months	VSD
19	256039	Female	1 year 1 month	VSD
20	255882	Male	6 months	VSD
21	256512	Male	1 years 4 months	VSD
22	257934	Female	1 years 2 months	VSD
23	258120	Female	1 years 4 months	VSD
24	258301	Male	7 months	VSD
25	258308	Female	3 years 7 months	VSD
26	258943	Male	7 months	VSD
27	259135	Male	2 years	VSD
28	259336	Male	4 years	VSD
29	228165	Female	1 years 5 months	TOF
30	228107	Female	8 months	TOF

VSD = ventricular septal defect; PAVC = partial atrioventricular canal defect; ASD = atrial septal defect; TGA = transposition of the great arteries; TOF = tetralogy of fallot.